Physiologia Plantarum
An International Journal for Plant Biology

Physiologia Plantarum 160: 155–170. 2017 ISSN 0031-9317

Two Southern Ocean diatoms are more sensitive to ocean acidification and changes in irradiance than the prymnesiophyte *Phaeocystis antarctica*

Scarlett Trimborn[a,b,*], Silke Thoms[a], Tina Brenneis[a], Jasmin P. Heiden[a,b], Sara Beszteri[a] and Kai Bischof[b]

[a]Department of Biogeosciences, Alfred Wegener Institute for Polar and Marine Research, Bremerhaven, 27515, Germany
[b]Marine Botany, University of Bremen, Bremen, Germany

Correspondence
*Corresponding author,
e-mail: Scarlett.Trimborn@awi.de

Received 15 November 2016;
revised 24 November 2016

doi:10.1111/ppl.12539

To better understand the impact of ocean acidification (OA) and changes in light availability on Southern Ocean phytoplankton physiology, we investigated the effects of pCO_2 (380 and 800 µatm) in combination with low and high irradiance (20 or 50 and 200 µmol photons m^{-2} s^{-1}) on growth, particulate organic carbon (POC) fixation and photophysiology in the three ecologically relevant species *Chaetoceros debilis*, *Fragilariopsis kerguelensis* and *Phaeocystis antarctica*. Irrespective of the light scenario, neither growth nor POC per cell was stimulated by OA in any of the tested species and the two diatoms even displayed negative responses in growth (e.g. *C. debilis*) or POC content (e.g. *F. kerguelensis*) under OA in conjunction with high light. For both diatoms, also maximum quantum yields of photosystem II (F_v/F_m) were decreased under these conditions, indicating lowered photochemical efficiencies. To counteract the negative effects by OA and high light, the two diatoms showed diverging photoacclimation strategies. While cellular chlorophyll a (Chl *a*) and fucoxanthin contents were enhanced in *C. debilis* to potentially maximize light absorption, *F. kerguelensis* exhibited reduced Chl *a* per cell, increased disconnection of antennae from photosystem II reaction centers and strongly lowered absolute electron transport rates (ETR). The decline in ETRs in *F. kerguelensis* might be explained in terms of different species-specific strategies for tuning the available flux of adenosine triphosphate and nicotinamide adenine dinucleotide phosphate. Overall, our results revealed that *P. antarctica* was more tolerant to OA and changes in irradiance than the two diatoms, which may have important implications for biogeochemical cycling.

Abbreviations – α, maximum light utilization efficiency; ATP, adenosine triphosphate; CCM, CO_2 concentrating mechanism; Chl *a*, chlorophyll a; Chl c_2, chlorophyll c_2; CO_2, carbon dioxide; Dd, diadinoxanthin; Dt, diatoxanthin; ETR, absolute electron transport rate; ETR_{max}, maximum absolute electron transport rate; Fuco, fucoxanthin; e^-, electron; GF/F, glassfibre filters; HPLC, high performance liquid chromatography; F′, light-adapted minimum fluorescence; F_o, minimum fluorescence; FLC, fluorescence light curve; F_m, maximum fluorescence; F′, light-adapted maximum fluorescence; F_q'/F_m', effective photosystem II quantum yield under ambient light; FRRf, fast repetition rate fluorometer; F_v/F_m, dark-adapted maximum photosystem II quantum yield; H^+, proton; I_K, minimum saturating irradiance; NADH, nicotinamide adenine dinucleotide; NADPH, nicotinamide adenine dinucleotide phosphate; NPQ, nonphotochemical quenching; OA, ocean acidification; *p*, dark-adapted connectivity; pCO_2, carbon dioxide partial pressure; POC, particulate organic carbon; PON, particulate organic nitrogen; PSII, photosystem II; [RII], concentration of functional photosystem II reaction centers; RubisCO, Ribulose-1,5-bisphosphate carboxylase/oxygenase; σ_{PSII}, dark-adapted functional absorption cross section of photosystem II photochemistry; τ, dark-adapted re-oxidation of the electron acceptor Q_a.

Introduction

Atmospheric carbon dioxide (CO_2) concentrations are projected to increase from about 390 μatm today beyond 750 μatm by the end of this century (IPCC 2014). The dissolution of additional atmospheric CO_2 into seawater alters the inorganic carbon buffer system by increasing the pCO_2 and decreasing the pH (IPCC 2014), potentially affecting phytoplankton physiology in various ways (Gao and Campbell 2014, Mackey et al. 2015). As CO_2 also acts as a greenhouse gas, it also causes the rise of global average temperatures (IPCC 2014), the warming and freshening of Southern Ocean surface waters will strengthen vertical stratification and reduce mixed-layer depth, which in turn will elevate mean solar irradiances phytoplankton cells encounter. Opposed to this scenario, it is also debated whether the occurrence of stronger westerly winds could increase and deepen vertical mixing of the upper surface layer (Hauck et al. 2015), thereby reducing mean irradiances with subsequent implications for Southern Ocean phytoplankton growth.

At present, investigations mainly aimed to resolve how Southern Ocean phytoplankton will respond to ocean acidification (OA) alone whereas the combined effect of OA with other environmental factors such as light availability is still poorly understood. For various Antarctic diatoms (*Chaetoceros brevis*, *Chaetoceros debilis*, *Rhizosolenia* cf. *alata*, *Pseudo-nitzschia subcurvata* and *Proboscia alata*) and the prymnesiophyte *P. antarctica*, growth and/or carbon fixation remained unaltered by OA alone (Boelen et al. 2011, Hoppe et al. 2015, Hoogstraten et al. 2012a, Riebesell et al. 1993, Trimborn et al. 2013). Only in the Antarctic sea ice diatom *Nitzschia lecointei*, growth was slightly stimulated from ambient to high pCO_2 levels in short-term experiments (Torstensson et al. 2013), but long-term acclimation (~200 days) under these conditions resulted also in a reduction in growth by 3–4% (Torstensson et al. 2015). Hence, OA alone did not alter growth or carbon fixation in the Southern Ocean phytoplankton tested so far. The reason for this may rely on the fact that carbon fixation rates of various Southern Ocean phytoplankton species are already close to saturation under present-day pCO_2 levels (Kranz et al. 2015, Trimborn et al. 2013, Young et al. 2015a). Therefore, one may expect beneficial CO_2 effects on growth and/or carbon fixation rather in combination with growth limiting conditions such as light limitation. In this case, the OA-dependent downregulation of the CO_2 concentrating mechanism (CCM), which elevates the concentration of CO_2 at the site of fixation by Ribulose-1,5-bisphosphate carboxylase/oxygenase (RubisCO), implies lower energy expenditures for CCM operation and therefore enables enhanced carbon fixation rates and/or growth particularly under low light conditions (Hopkinson et al. 2011). In line with this, several temperate diatom species displayed stimulation in growth under OA and low light (Li and Campbell 2013, Li et al. 2014, McCarthy et al. 2012). Such responses were, however, not reported for the Antarctic diatoms *P. alata* (Hoogstraten et al. 2012a) and *C. brevis* (Boelen et al. 2011), which both exhibited no OA-dependent change in growth rates in response to limiting or saturating irradiance levels. OA in combination with high light, however, resulted in light stress and photodamage with inhibitory effects on growth of several temperate phytoplankton species (Chen and Gao 2011, Gao et al. 2012, Hoogstraten et al. 2012b, Li and Campbell 2013). Even though phytoplankton potentially benefit from reduced operational costs of the CCM under OA, high pCO_2 may also prevent the CCM to act as an energy sink under high light conditions. Therefore, OA may lead to a higher susceptibility toward photoinhibition, which needs to be counteracted by a higher capacity for photosystem II repair (McCarthy et al. 2012). Whether Southern Ocean phytoplankton will physiologically respond in a similar way to OA in combination with different light availability remains, however, at present unclear and still needs further investigation.

Depending on light availability, the phytoplankton cell needs to balance between light absorption for energy generation and energetic costs for cell maintenance whereas under high light the prevention of potential damage of photosystem II (PSII) can be necessary. To protect PSII from overexcitation, Southern Ocean diatoms and *P. antarctica* rely on xanthophyll cycle-dependent nonphotochemical quenching (NPQ, Kropuenske et al. 2010, Mills et al. 2010, Trimborn et al. 2014, Van de Poll et al. 2011). If PSII photoinactivation outruns the rate of repair, the PSII pool suffers net photoinhibition (Li and Campbell 2013, Murata et al. 2007, Raven 2011), leading ultimately to a decrease in photosynthetic capacity. In particular under high light conditions combined with OA, temperate diatoms were susceptible for photoinactivation of their PSII reaction centers, (Chen and Gao 2011, Gao et al. 2012, McCarthy et al. 2012, Li and Campbell 2013) whereas information for prymnesiophytes is still missing under these conditions. Studies have shown that strong taxon-specific differences in photophysiology between diatoms and prymnesiophytes exist in response to changes in irradiance (Arrigo et al. 2010, Kropuenske et al. 2010, Mills et al. 2010, Van de Poll et al. 2011). According to these studies, the diatoms *Fragilariopsis cylindrus* and *C. brevis* were better protected from photoinhibition under high light levels as typically occurring in regions with a shallow mixed layer depth. In comparison, *P. antarctica* was able to efficiently

Table 1. Parameters of the seawater carbonate system were calculated from alkalinity, pH, silicate, phosphate, temperature and salinity using the CO2Sys program (Pierrot et al. 2006).

Target pCO_2 (μatm)	pCO_2 (μatm)	CO_2 (μmol kg^{-1})	DIC (μmol kg^{-1})	TA (μmol kg^{-1})	pH (NBS)
Ambient, 390	360 ± 20	20 ± 1	2089 ± 12	2225 ± 17	8.17 ± 0.03
High, 800	824 ± 67	47 ± 4	2185 ± 20	2235 ± 13	7.83 ± 0.03

use light in particular under low irradiance levels as in a deeply mixed water column. As diatoms and prymnesiophytes are generally considered key drivers for biogeochemical cycling with diatoms predominantly regulating the carbon (Smetacek 1999) and silicon cycle (Tréguer 2002) and *P. antarctica* the marine sulfur cycle (Liss et al. 1994), it is crucial to understand how both taxonomic groups will be influenced under the different future OA and light scenarios.

In this study, the two diatoms *C. debilis* and *Fragilariopsis kerguelensis* and the prymnesiophyte *P. antarctica*, being relevant in both ecological as well as biogeochemical terms, were grown under OA to test the modulating effect of light intensity on their physiological responses. To this end, all species were grown under two pCO_2 levels (380 and 800 μatm) in combination with two irradiance levels (20 or 50 and 200 μmol photons m^{-2} s^{-1}) and their interactive effects on growth, carbon fixation and photophysiology were assessed.

Materials and methods

Culture conditions

The two diatoms *C. debilis* (Polarstern expedition 'EIFEX' ANT-XXI/3, In-Patch, 2004, 49°36 S, 02°05°E, isolated by Philipp Assmy) and *F. kerguelensis* (Polarstern expedition ANT-XXIV/2 in 2008 at 64°S, 0°E, isolated by Philipp Assmy) and the flagellate *Phaeocystis antarctica* (solitary cells isolated by P. Pendoley in March 1992 at 68°39°S, 72°21°E) were grown at 2°C in semi-continuous cultures in sterile-filtered (0.2 μm) Antarctic seawater (salinity 33.2 psu). The seawater was enriched with trace metals and vitamins according to F/2 medium (Guillard and Ryther 1962). Phosphate and nitrate were added in concentrations of 100 and 6.25 μmol l^{-1}, reflecting the Redfield N:P ratio of 16:1 (Redfield 1958). Cultures as well as the respective dilution media were continuously and gently bubbled through a frit with humidified air of CO_2 partial pressures (pCO_2) of 380 and 800 μatm, resulting in pH values of 8.17 and 7.83, respectively (ambient and high pCO_2 treatment, Table 1). CO_2 gas mixtures were generated with a gas flow controller (CGM 2000, MCZ Umwelttechnik, Bad Nauheim, Germany), using CO_2-free air (<1 ppmv CO_2; Dominick Hunter, Kaarst, Germany) and pure CO_2 (Air Liquide Deutschland ltd., Düsseldorf, Germany). The CO_2 gas mixtures were regularly monitored with a nondispersive infrared analyzer system (LI6252; Li-Cor Biosciences, Lincoln, NE) calibrated with CO_2-free air and purchased gas mixtures of 150 ± 10 and 1000 ± 20 ppmv CO_2 (Air Liquide Deutschland ltd., Düsseldorf, Deutschland). Daily dilutions with the corresponding acclimation media ensured that the pH remained constant (±0.03, Table 1) and that the cells stayed in the mid-exponential growth phase. In addition to different pCO_2 levels, the 3 species were grown in triplicates at an incident light intensity of 20 and 200 μmol photons m^{-2} s^{-1} (low and high light treatment) under a light:dark cycle of 16:8 h. As *F. kerguelensis* did not grow between 20 and 40 μmol photons m^{-2} s^{-1}, the low light treatment was increased up to 50 μmol photons m^{-2} s^{-1}. Light intensities were adjusted using a LI-1400 datalogger (Li-Cor Biosciences, Lincoln, NE) with a 4π-sensor (Walz, Effeltrich, Germany). The three phytoplankton species were acclimated to the respective light and pCO_2 levels for at least 2 weeks prior to sampling.

Determination of seawater carbonate chemistry

Alkalinity samples were taken from the filtrate (Whatman GF/F filter, ~0.6 μm), stored in 150-ml borosilicate flasks at 4°C and measured by potentiometric titration (Brewer et al. 1986). Total alkalinity was calculated from linear Gran Plots (Gran 1952). pH was measured using a pH meter (WTW, model pMX 3000/pH, Weilheim, Germany) that was calibrated on a daily basis (3-point calibration) using National Institute of Standards and Technology-certified buffer systems. The carbonate system was calculated from alkalinity, pH, silicate, phosphate, temperature and salinity using the CO2Sys program (Pierrot et al. 2006). Equilibrium constants of Mehrbach et al. (1973) refitted by Dickson and Millero (1987) were chosen. The parameters of the carbonate system for the respective treatments are given in Table 1.

Growth, elemental stoichiometry and composition

Cell count samples were taken on a daily basis at the same time of day. While cell numbers for *P. antarctica* were determined immediately after sampling using a

Coulter Multisizer III (Beckmann-Coulter, Fullerton, CA), cell count samples of *C. debilis* were fixed with 10% acid Lugol's solution and stored at 2°C in the dark until counting. Cell numbers of *C. debilis* were estimated according to the method by Utermöhl (1958) using 10 ml sedimentation chambers (Hydrobios, Kiel, Germany) on an inverted microscope (Zeiss Axiovert 200) counting at least 400 cells in transects. Cell-specific growth rate (μ, day^{-1}) was calculated as

$$\mu = \left(\ln N_{fin} - \ln N_0\right) / \Delta t \quad (1)$$

where N_0 and N_{fin} denote the cell concentrations at the beginning and the end of the experiments, respectively, and Δt is the corresponding duration of incubation in days. As in case of *C. debilis*, cell count samples of *F. kerguelensis* were fixed and stored at 2°C in the dark. Due to the formation of long chains and the heterogeneity of *F. kerguelensis* cells within the chamber after sedimentation, *F. kerguelensis* cells were enumerated two times in the whole chamber. As the counting was very time intensive, cell abundances of *F. kerguelensis* were solely quantified for the start of the experiment and the final sampling. To still derive growth rates, the in vivo chlorophyll *a* (Chl *a*) fluorescence of the *F. kerguelensis* cells were measured on a daily basis on a Turner Designs fluorometer (Model 10-000 R, Mt. View, Canada). As the in vivo fluorescence was too low in the high light treatments, Chl *a*-specific growth rates were only estimated for the low light treatments of *F. kerguelensis*.

Particulate organic carbon (POC) and particulate organic nitrogen (PON) were measured after filtration onto precombusted (15 h, 500°C) glassfiber filters (GF/F, pore size ~0.6 µm, Whatman). Filters were stored at −20°C and dried for >12 h at 60°C prior to sample preparation. Analysis was performed using a Euro Vector CHNS-O elemental analyzer (Euro Elemental Analyzer 3000, HEKAtech GmbH, Wegberg, Germany). Contents of POC and PON were corrected for blank measurements and normalized to filtered volume and cell densities to yield cellular quotas.

Pigment concentration and composition

Samples for the determination of pigment concentration were filtered onto GF/F filters and stored at −80°C until analysis. Pigments samples were homogenized and extracted in 90% acetone for 24 h at 4°C in the dark. After centrifugation (5 min, 4°C, 7747 *g*) and filtration through a 0.45 µm pore size nylon syringe filter (Nalgene®, Nalge Nunc International, Rochester, NY), concentrations of chlorophyll *a* (Chl *a*) and c_2 (Chl c_2), fucoxanthin (Fuco), diatoxanthin (Dt) and diadinoxanthin (Dd) were determined by reversed phase High Performance Liquid Chromatography (HPLC). The analysis was performed on a LaChromElite® system equipped with a chilled autosampler L-2200 and a DAD detector L-2450 (VWR-Hitachi International GmbH, Darmstadt, Germany). A Spherisorb® ODS-2 column (25 cm × 4.6 mm, 5 µm particle size; Waters, Milford, MA) with a LiChropher® 100-RP-18 guard cartridge was used for the separation of pigments, applying a gradient according to Wright et al. (1991). Peaks were detected at 440 nm and identified as well as quantified by co-chromatography with standards for Chl *a* and c_2, Fuco, Dt, and Dd (DHI Lab Products, Hørsholm, Denmark) using the software EZCHROM ELITE ver. 3.1.3. (Agilent Technologies, Santa Clara, CA). Pigment contents were normalized to filtered volume and cell densities to yield cellular quotas.

Chlorophyll *a* fluorescence

Chlorophyll *a* fluorescence of PSII was assessed in cells of all treatments using a Fast Repetition Rate fluorometer (FRRf, FastOcean PTX; Chelsea Technologies Group ltd., West Molesey, UK) in combination with a FastAct Laboratory system (Chelsea Technologies Group ltd., West Molesey, UK). Cells of the respective treatment were transferred to the cuvette of the FRRf system and dark-adapted for 10 min, before minimum fluorescence (F_o) was recorded. This dark-adaptation period was chosen after testing different time intervals (5, 10, 15, 20 and 30 min) prior to measurements to ensure largest possible F_m. A single turnover flashlet (1.2×10^{22} photons m^{-2} s^{-1}, wavelength 450 nm) was then applied to cumulatively saturate PSII, i.e. a single photochemical turnover (Kolber et al. 1998). The single turnover saturation phase comprised 100 flashlets on a 2 µs pitch and was followed by a relaxation phase comprising 40 flashlets on a 50 µs pitch. This sequence was repeated 24 times within each acquisition. The saturation phase of the single turnover acquisition was fitted according to Kolber et al. (1998). From this measurement, the minimum (F_o) and maximum (F_m) fluorescence was determined. Using these two parameters, the dark-adapted maximum PSII quantum yield (F_v/F_m) was calculated according to the equation $(F_m - F_o)/F_m$. During the fluorescence light curve (FLC), cells were exposed for 5 min to eight actinic light levels ranging from 24 to 1700 µmol photons m^{-2} s^{-1}. From these measurements, the light-adapted minimum (F') and maximum (F_m') fluorescence of the single turnover acquisition was estimated. The effective PSII quantum yield under ambient light (F_q'/F_m') was derived according to the equation $(F_m' - F')/F_m'$ (Genty et al. 1989). From this curve, absolute electron transport

rates (ETR, $e^- PSII^{-1} s^{-1}$) were calculated following Suggett et al. (2004, 2009):

$$ETR = \sigma_{PSII} \times \left(\left(F_q'/F_m' \right) / \left(F_v/F_m \right) \right) \times E \quad (2)$$

where σ_{PSII} is the functional absorption cross section of PSII photochemistry and E denotes the instantaneous irradiance (photons m^{-2} s^{-1}). Light-use characteristics were analyzed by fitting irradiance-dependent ETRs according to Ralph and Gademann (2005), including maximum ETR (ETR_{max}), minimum saturating irradiance (I_K) and maximum light utilization efficiency (α). Using the Stern-Volmer equation, nonphotochemical quenching (NPQ) of chlorophyll *a* fluorescence was calculated as $F_m/F_m' - 1$. From the single turnover measurement of dark-adapted cells, σ_{PSII}, the energy transfer between PSII units (i.e. connectivity, *p*), the re-oxidation of the electron acceptor Q_a (τ) and the concentration of functional photosystem II reaction centers [RII] were assessed from iterative algorithms for induction (Kolber et al. 1998) and relaxation phase (Oxborough 2012). [RII] represents an estimator for the content of PSII in the sample and was calculated according to the following equation:

$$[RII] = \left(F_o / \sigma_{PSII} \right) \times \left(K_R / E_{LED} \right) \quad (3)$$

where K_R is an instrument specific constant and E_{LED} is the photon flux from the FRRf measuring LEDs. After the completion of the light curve, an additional dark-adaptation period of 10 min was applied, followed by a single turnover flashlet to check for recovery of PSII. All measurements ($n \geq 4$) were conducted at the growth temperature of 2°C.

Statistics

Interactive effects of the two pCO_2 (ambient and high) and light treatments (low and high) on all experimental parameters were statistically analyzed using two-way ANOVA with Bonferroni's multiple comparison post tests. Statistical analyses were performed using the program GraphPad Prism (Version 5.00 for Windows, Graph Pad Software, San Diego, CA). All significance testing was done at the $P < 0.05$ level.

Results

Growth, elemental composition and stoichiometry

Growth of the tested species was differently affected by light and pCO_2 (Fig. 1A–C). High light significantly increased growth rates of *C. debilis* by 110% under ambient pCO_2 (post hoc: $P < 0.001$) and by 112% under high pCO_2 (post hoc: $P < 0.001$). A similar pattern was observed for *P. antarctica*, but with a less pronounced light-dependent stimulation in growth by 10 (post hoc: $P > 0.05$) and 47% (post hoc: $P < 0.05$) under ambient and high pCO_2, respectively. Growth was generally not altered by elevated pCO_2, except for *C. debilis*. In the latter, growth declined with increasing pCO_2 by 18% under low light (post hoc: $P > 0.05$) and by 17% under high light (post hoc: $P > 0.05$).

Cellular quotas of POC and particulate organic nitrogen (PON) were generally not affected by high light and elevated pCO_2 (Fig. 1D–F). The only exception was *F. kerguelensis*, for which POC per cell significantly increased with increasing light: fivefold under ambient pCO_2 (post hoc: $P < 0.0001$) and doubled under high pCO_2 (post hoc: $P < 0.01$). While POC per cell of low light acclimated *F. kerguelensis* cells remained unaltered in response to elevated pCO_2, the cellular POC content was reduced by 60% in high light acclimated cells (post hoc: $P < 0.0001$). Cellular quotas of PON exhibited the same trends as observed for POC, with no effect in response to high light and elevated pCO_2 in *P. antarctica* and *C. debilis* and strong effects in *F. kerguelensis* (data not shown). Ratios of C:N did not change in response to high light or to elevated pCO_2 in the tested species (Fig. 1G–I).

Chlorophyll *a* fluorescence

The dark-acclimated maximum quantum yield of PSII (F_v/F_m) remained unaltered in response to high light and elevated pCO_2 in *P. antarctica*, but changed in *C. debilis* and *F. kerguelensis* (Fig. 2A–C). With increasing light, F_v/F_m was not altered under ambient pCO_2 whereas under elevated pCO_2 it was reduced by 17% in *C. debilis* (post hoc: $P < 0.001$) and by 20% in *F. kerguelensis* (post hoc: $P < 0.001$). Elevated pCO_2 had further an effect on F_v/F_m, but only at high light, reducing the yield by 10% in *C. debilis* (post hoc: $P < 0.05$) and by 17% in *F. kerguelensis* (post hoc: $P < 0.05$).

Recovery of F_v/F_m strongly differed among species (Fig. 2D–F). While high light significantly enhanced the recovery of the photosynthetic yield by 176% in *P. antarctica* (post hoc: $P < 0.0001$) and by 22% in *F. kerguelensis* (post hoc: $P < 0.001$) under ambient pCO_2, the yield recovery was unaltered at high pCO_2. In *C. debilis* on the other hand, high light resulted in a decrease of the yield recovery by 20% under ambient pCO_2 (post hoc: $P < 0.001$) whereas under high pCO_2 the recovery was enhanced by 60% (post hoc: $P < 0.0001$). In *P. antarctica*, elevated pCO_2 increased the recovery of the yield by 105% under low (post hoc: $P < 0.01$), but not under high light. Opposite to this, in *C. debilis* the yield recovery declined with increasing pCO_2 by 55% under low light

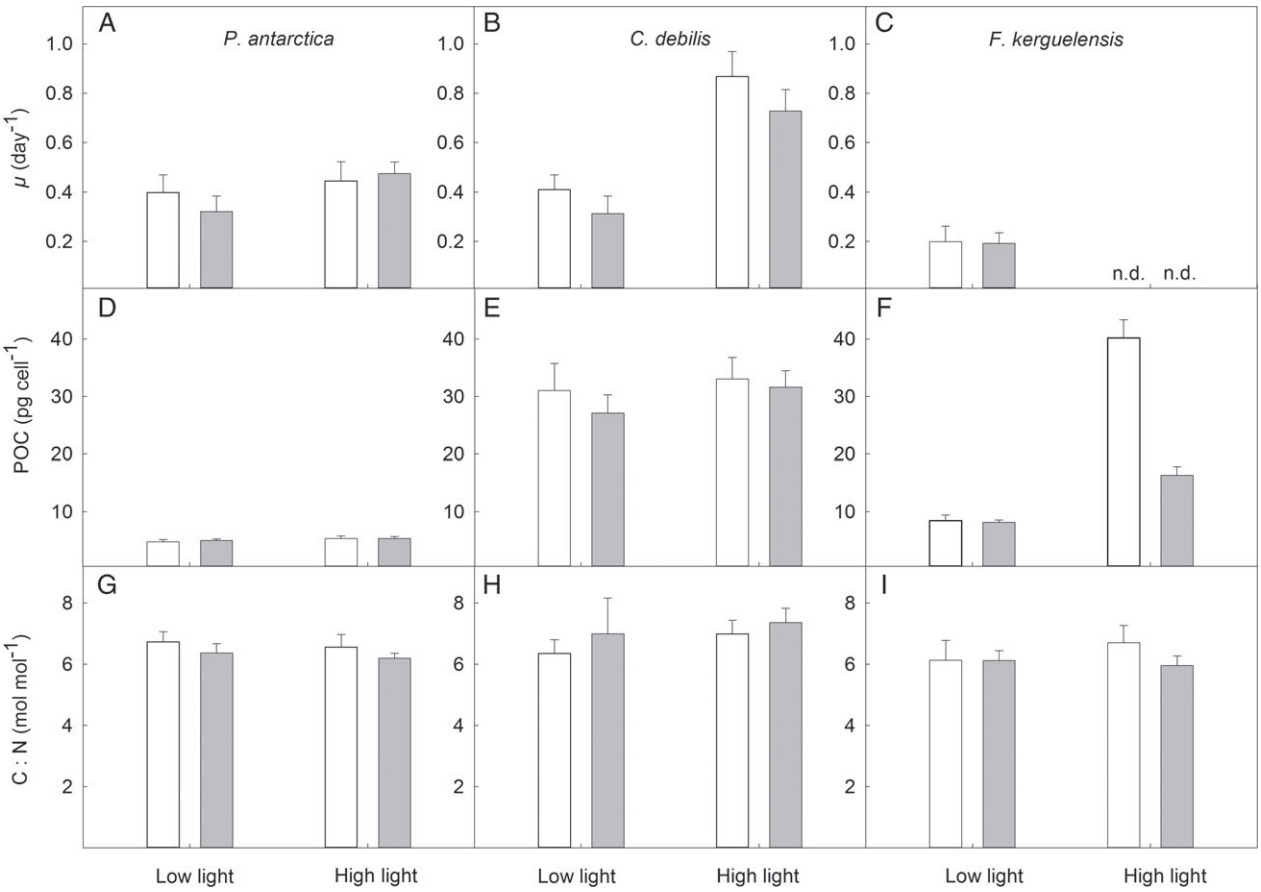

Fig. 1. Growth rates (μ, in day^{-1}), particulate organic carbon content (POC, in pg cell^{-1}) and C:N molar ratios for *Phaeocystis antarctica* (A, D, G), *Chaetoceros debilis* (B, E, H) and *Fragilariopsis kerguelensis* (C, F, I) acclimated to ambient (white bars) and high (grey bars) pCO_2 combined with low and high light. For *F. kerguelensis*, growth rates of the HL acclimation could not be determined (n.d.). Values represent the means ± SD ($n \geq 3$).

(post hoc: $P < 0.0001$), but remained unaltered under high light. In *F. kerguelensis*, elevated pCO_2 did not alter the yield recovery under low light, but led to a significant decline by 19% under high light (post hoc: $P < 0.001$).

Fluorescence light curves showed clear species-specific differences in both shape and amplitude in response to high light and elevated pCO_2 (Fig. 3). Maximum absolute electron transport rates (ETR_{max}) generally increased with increasing light under both pCO_2 levels (Table 2). The only exception was the high pCO_2 treatment of *F. kerguelensis*, which showed a significant decline in ETR_{max} by 46% with increasing light (post hoc: $P < 0.0001$). Within the same light level, ETR_{max} declined in response to elevated pCO_2 in both light treatments of *C. debilis* ($P < 0.01$) as well as in the high light treatment of *F. kerguelensis* (post hoc: $P < 0.0001$). The minimum saturating irradiance (I_K) generally increased with increasing irradiance except for the high pCO_2 treatment of *F. kerguelensis* (Table 2). Among species, I_K was differently affected by elevated pCO_2. For *P. antarctica* and *C. debilis*, I_K remained unaltered in response to elevated pCO_2 in both light treatments. Only for the high light acclimation of *F. kerguelensis*, a strong CO_2-dependent decline by 64% (post hoc: $P < 0.0001$) was observed. The maximum light utilization efficiency (α) was differently affected by high light in the tested species (Table 2). For *P. antarctica*, α significantly increased in response to high light by 25 (post hoc: $P < 0.01$) and 38% (post hoc: $P < 0.001$) in the ambient and high pCO_2 treatment, respectively. Similarly, for *F. kerguelensis*, α showed a light-dependent increase by 35% at ambient pCO_2 (post hoc: $P < 0.01$), but a significant decline by 28% at elevated pCO_2 (post hoc: $P < 0.01$). Opposed to this, α remained unaltered in response to high light in the ambient pCO_2 treatment of *C. debilis*, but also decreased by 20% in the high pCO_2 treatment (post hoc: $P < 0.01$). Within the same light level, α values did generally not change in response to elevated pCO_2 in the tested species. Only for low-light acclimated cells of *C. debilis*, a CO_2-dependent

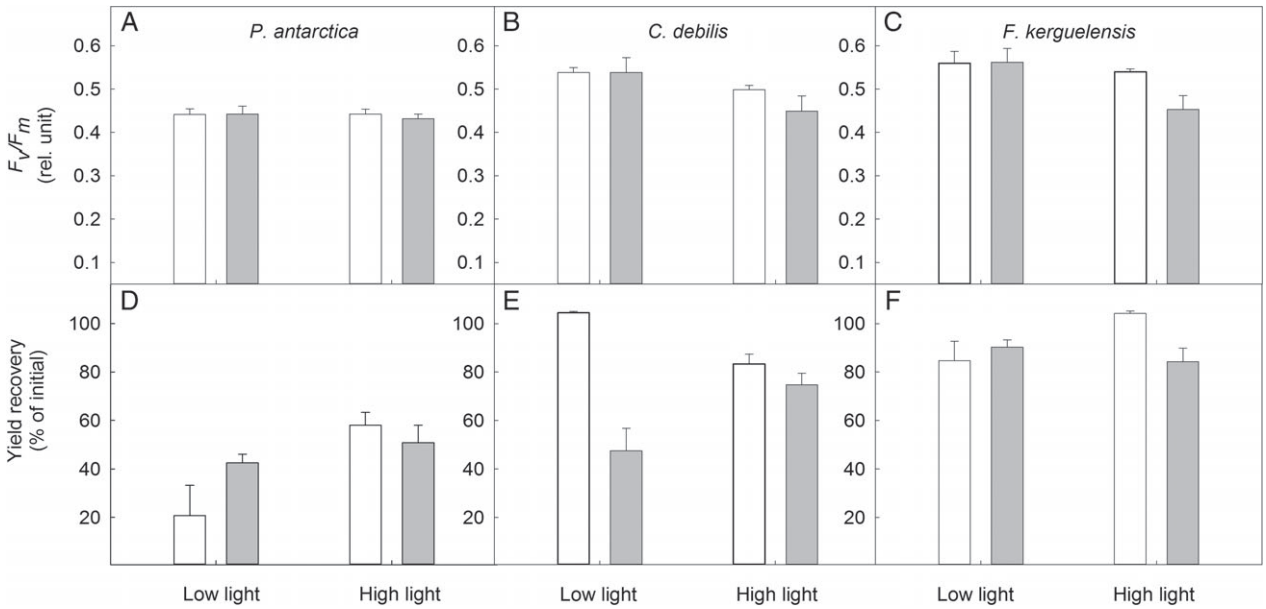

Fig. 2. The dark-adapted maximum PSII quantum yield (F_v/F_m, rel. unit) and the yield recovery after short-term light stress (% of initial) for *Phaeocystis antarctica* (A, D), *Chaetoceros debilis* (B, E) and *Fragilariopsis kerguelensis* (C, F) acclimated to ambient (white bars) and high (grey bars) pCO_2 combined with low and high light. Values represent the means ± SD ($n \geq 4$).

increase in α by 20% was observed (post hoc: $P < 0.05$). Furthermore, α was significantly lowered by 47% at elevated pCO_2 in high light acclimated cells of F. *kerguelensis* (post hoc: $P < 0.0001$).

The functional absorption cross-section of PSII (σ_{PSII}) was differently affected by high light in the tested species (Table 2). In *P. antarctica*, high light significantly increased σ_{PSII} under both pCO_2 levels (ANOVA: $P < 0.0001$) whereas σ_{PSII} was significantly decreased under these conditions in *C. debilis* (ANOVA: $P < 0.001$). Only for *F. kerguelensis*, σ_{PSII} remained unchanged in response to high light. For all species, elevated pCO_2 had no effect on σ_{PSII}. Concentrations of functional photosystem II reaction centers, [RII] showed species-specific differences in response to high light (Table 2). While in *P. antarctica* [RII] significantly declined by 51 (ANOVA: $P < 0.01$) and 61% (ANOVA: $P < 0.001$) in response to high light under ambient and high pCO_2, respectively, in *C. debilis* [RII] significantly increased by 411% in the ambient pCO_2 treatment (ANOVA: $P < 0.0001$), but remained unaltered in the high pCO_2 treatment. In comparison, [RII] was unaltered by high light in *F. kerguelensis*. In response to elevated pCO_2, [RII] did not change in any light treatment of *P. antarctica* and *F. kerguelensis*. Only in high light acclimated cells of *C. debilis,* [RII] showed a significant CO_2-dependent decrease by 83% (ANOVA: $P < 0.0001$). The re-oxidation of the primary electron acceptor Q_a (τ) did not change in response to high light in *C. debilis* and *F. kerguelensis* (Table 2). Opposed to this, high light acclimated cells of *P. antarctica* had much shorter re-oxidation times than low-light acclimated cells (ANOVA: $P < 0.0001$). In response to elevated pCO_2, τ values generally remained unaltered. The energy transfer between PSII units (i.e. connectivity, *p*) strongly varied in response to high light and elevated pCO_2 among species (Table 2). In *P. antarctica*, a significant light-dependent increase in *p* by 175 (post hoc: $P < 0.001$) and 160% (post hoc: $P < 0.01$) was observed in low and high light acclimated cells, respectively. In comparison, *p* did not change in response to high light in low and high pCO_2 acclimated cells of *C. debilis*. For *F. kerguelensis*, high light did also not affect *p* in cells grown under ambient pCO_2, but strongly decreased *p* in cells grown under elevated pCO_2 (post hoc: $P < 0.01$). The acclimation pCO_2 did generally not alter *p*. The only exceptions were the high light treatments, in which *p* significantly decreased in response to elevated pCO_2 by 18% in *C. debilis* (post hoc: $P < 0.05$) and by 43% in *F. kerguelensis* (post hoc: $P < 0.01$).

In all species, nonphotochemical quenching (NPQ) generally went up with increasing actinic irradiance during the fluorescence irradiance (FLC) curve (Fig. 4). With respect to the acclimation irradiance (low vs high), NPQ values generally remained unaltered. Only for *P. antarctica*, NPQ values of the high light treatments were generally higher relative to those of the low light treatments. Moreover, the acclimation pCO_2 did not affect NPQ, apart from the high light treatment of

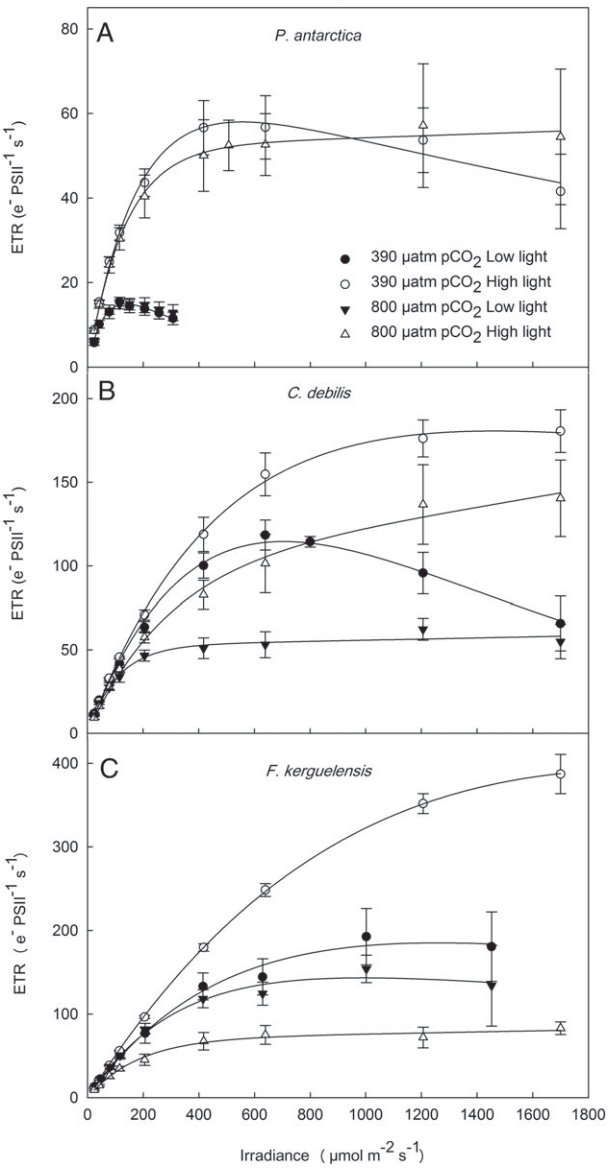

Fig. 3. Electron transport rates (ETR, in e^{-} $PSII^{-1}$ s^{-1}) were determined in response to increasing irradiance in (A) *Phaeocystis antarctica*, (B) *Chaetoceros debilis* and (C) *Fragilariopsis kerguelensis* acclimated to ambient (circles) and high (triangles) pCO_2 combined with low (filled) and high (open) light. ETRs were obtained in at least four individual measurements. Values represent the means ± SD ($n \geq 4$).

F. kerguelensis, which showed lowered NPQ values relative to those of the other treatments.

Cellular pigment concentrations

Chl *a* per cell was differently affected by high light in the tested species (Table 3). High light strongly decreased Chl *a* per cell of *P. antarctica* and *C. debilis* within the same pCO_2 treatment (ANOVA: $P < 0.0001$). Opposed to this, Chl *a* per cell of *F. kerguelensis* significantly increased by 153% in response to high light in the ambient pCO_2 treatment (post hoc: $P < 0.0001$) whereas it remained constant in the high pCO_2 treatment. In response to elevated pCO_2, Chl *a* per cell was generally not affected among species. Only for the high light treatments, Chl *a* per cell significantly increased with increasing pCO_2 during acclimation by 153% in *C. debilis* (post hoc: $P < 0.01$) whereas it significantly declined by 73% in *F. kerguelensis* (post hoc: $P < 0.01$). Cellular Chl c_2 concentrations generally were not altered by high light (Table 3). For the high pCO_2 treatments of *P. antarctica*, however, Chl c_2 per cell significantly declined with increasing light (post hoc: $P < 0.05$) whereas the ambient pCO_2 treatments of *F. kerguelensis* were characterized by a significant increase in this parameter (post hoc: $P < 0.05$). In response to elevated pCO_2, Chl c_2 per cell generally remained constant except for the high light acclimated *F. kerguelensis* cells that showed a decline by 56% under these conditions. Cellular fucoxanthin (Fuco) concentrations significantly decreased with increasing light within the same pCO_2 acclimation of *P. antarctica* (ANOVA: $P < 0.0001$) and *C. debilis* (ANOVA: $P < 0.0001$) whereas they remained unchanged in *F. kerguelensis* (Table 3). For all species, the acclimation to different pCO_2 did not alter cellular Fuco contents. High light differently affected cellular concentrations of Dd of the different species (Table 3). For *P. antarctica*, Dd per cell increased with increasing light in both pCO_2 treatments (ANOVA: $P < 0.0001$). In comparison, Dd per cell remained unaffected by high light in the ambient pCO_2 treatment of *C. debilis*, but increased by 33% in the high pCO_2 treatment (post hoc: $P < 0.05$). Opposed to this, cellular Dd concentrations were only enhanced in response to high light in the ambient pCO_2 treatment of *F. kerguelensis* (post hoc: $P < 0.05$), but remained constant in the high pCO_2 treatment. For all species, cellular Dd contents were not changed in response to elevated pCO_2. Ratios of protective: light harvesting pigments generally increased in response to high light (for *P. antarctica*: ANOVA: $P < 0.0001$, for *C. debilis*: ANOVA: $P < 0.05$) except for *F. kerguelensis* (Table 3). In the latter, ratios were not changed by high light. With regard to changes in pCO_2 during acclimation, ratios of protective: light harvesting pigments remained generally constant. Only for the high light acclimated cells of *P. antarctica*, ratios increased by 20% in response to increasing pCO_2 (post hoc: $P < 0.05$).

Discussion

Currently, information on interactive effects of OA and light is limited for Southern Ocean phytoplankton as

Table 2. Maximum absolute electron transport rates (ETR_{max}), minimum saturating irradiances (I_K), maximum light utilization efficiencies (α), concentrations of functional photosystem II reaction centers [RII], functional absorption cross-sections (σ_{PSII}), re-oxidation times of the primary electron acceptor Q_a (τ), and the energy transfer between photosystem II units (i.e. connectivity, *p*) were determined for *Phaeocystis antarctica*, *Chaetoceros debilis* and *Fragilariopsis kerguelensis* acclimated to ambient and high pCO_2 combined with low and high light. Photosynthetic parameters from photosynthesis irradiance curves were derived from at least four independent measurements.

Treatment	ETR_{max} (e^- $PSII^{-1}$ s^{-1})	I_k (μmol m^{-2} s^{-1})	α (rel. unit)	[RII] (nmol m^{-3})	σ_{PSII} (nm^2)	τ (μs)	*p* (rel. unit)
P. antarctica							
390 LL	15 ± 4	37 ± 5	0.40 ± 0.04	12.23 ± 2.03	5.13 ± 0.17	637 ± 30	0.12 ± 0.05
390 HL	78 ± 14	152 ± 19	0.50 ± 0.03	6.01 ± 0.62	5.68 ± 0.28	542 ± 27	0.33 ± 0.04
800 LL	18 ± 2	45 ± 4	0.39 ± 0.03	12.51 ± 2.83	5.16 ± 0.15	635 ± 30	0.10 ± 0.06
800 HL	70 ± 11	131 ± 20	0.54 ± 0.04	4.92 ± 1.33	5.85 ± 0.27	526 ± 29	0.26 ± 0.08
Cn debilis							
390 LL	94 ± 15	216 ± 40	0.41 ± 0.04	3.58 ± 0.80	4.88 ± 0.20	558 ± 24	0.50 ± 0.02
390 HL	167 ± 4	408 ± 28	0.39 ± 0.03	18.31 ± 4.50	4.39 ± 0.20	562 ± 22	0.45 ± 0.01
800 LL	51 ± 9	104 ± 22	0.49 ± 0.02	3.13 ± 1.26	5.12 ± 0.32	545 ± 34	0.44 ± 0.05
800 HL	118 ± 29	312 ± 118	0.39 ± 0.05	3.20 ± 1.44	4.50 ± 0.27	568 ± 28	0.37 ± 0.04
F. kerguelensis							
390 LL	151 ± 12	379 ± 36	0.43 ± 0.07	5.11 ± 1.05	4.90 ± 0.26	553 ± 40	0.39 ± 0.07
390 HL	412 ± 22	681 ± 64	0.58 ± 0.05	5.65 ± 2.15	5.16 ± 0.15	538 ± 34	0.43 ± 0.05
800 LL	134 ± 8	310 ± 37	0.43 ± 0.03	5.26 ± 2.19	4.95 ± 0.33	561 ± 45	0.42 ± 0.08
800 HL	72 ± 2	242 ± 20	0.31 ± 0.02	3.69 ± 1.18	4.29 ± 0.99	624 ± 67	0.24 ± 0.08

most studies either focused solely on either CO_2 (Riebesell et al. 1993, Trimborn et al. 2013, 2014) or the light intensity (Arrigo et al. 2010, Kropuenske et al. 2010, Robinson et al. 1997, Van Leeuwe et al. 2005), yet rarely on both (Boelen et al. 2011, Hoogstraten et al. 2012a). To better understand how phytoplankton will respond to the projected changes in pCO_2 and light in a future Southern Ocean, we investigated the combined effect of OA and light on growth, POC fixation and photophysiology in the three bloom-forming Southern Ocean phytoplankton species *P. antarctica*, *C. debilis* and *F. kerguelensis*. Our study indicates that the investigated species possess different physiological strategies to cope with OA under the different light scenarios and further reveals that the two tested diatom species are particularly sensitive compared with the prymnesiophyte.

OA did not stimulate growth or POC fixation under low light

Under OA combined with low light, temperate diatom species often exhibit an OA-dependent stimulation in growth (McCarthy et al. 2012, Li and Campbell 2013, Li et al. 2014). This phenomenon was ascribed to increased diffusive CO_2 uptake under OA counteracting the decreased capacity and/or affinity for inorganic carbon uptake (Kranz et al. 2010, Rokitta and Rost 2012, Beardall and Raven 2013) caused by energy limitation under low light (Giordano et al. 2005, Young and Beardall 2005, Raven et al. 2011). In our tested species, neither growth nor POC per cell was stimulated by OA under low light (Fig. 1). Also in *P. alata* (Hoogstraten et al. 2012a) and *P. globosa* (Hoogstraten et al. 2012b), growth remained constant under those conditions. Moreover, photochemical efficiencies of our tested species were not affected under low light combined with OA, as shown by the unaltered F_v/F_m (Fig. 2) and [RII] values (Table 2). When acclimated to low light and ambient pCO_2, *C. debilis* showed signs of dynamic photoinhibition during FLC-curves (Fig. 3), as suggested by its unchanged capacity to recover from short-term light stress, which accounted for ~100% (Fig. 2). The acclimation of *C. debilis* to OA and low light, however, led to reduced ability to recover from short-term light exposure (~80%, Fig. 2) and resulted further in a significant decline in both ETR_{max} and α (Fig. 3, Table 2), indicating a strongly reduced photosynthetic efficiency. The negative impact of OA even under low-light conditions on the photosynthetic capacity of *C. debilis* is surprising and has not yet been reported before. One may speculate whether the CCM of *C. debilis* was downregulated under OA to a lesser extent in the low light treatment compared with that under high light, as previously observed for the temperate diatom *P. tricornutum* (Li et al. 2014), implying higher energetic costs for CCM operation under these conditions. Overall, it is notable that the Southern Ocean phytoplankton species tested so far (our study, Hoogstraten et al. 2012a) did not show any OA-dependent stimulation in growth or POC fixation under low light, casting doubt on the beneficial effects of elevated pCO_2 for Southern Ocean phytoplankton species under these conditions.

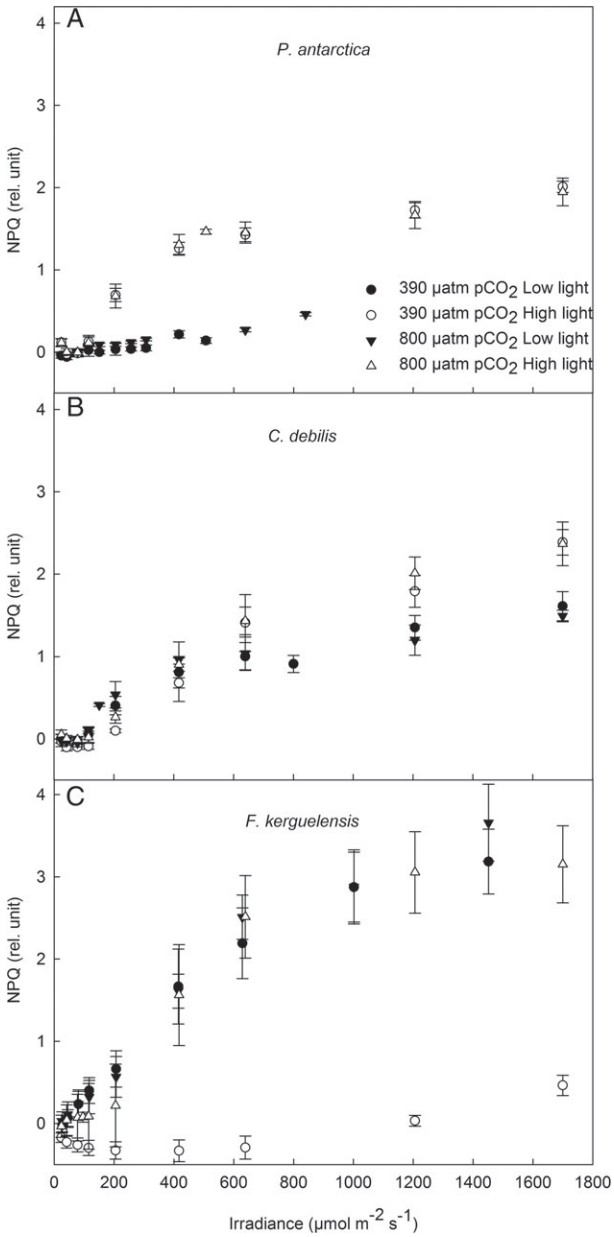

Fig. 4. Nonphotochemical quenching (NPQ, rel. unit) was determined in response to increasing irradiance in (A) *Phaeocystis antarctica*, (B) *Chaetoceros debilis* and (C) *Fragilariopsis kerguelensis* acclimated to ambient (circles) and high (triangles) pCO_2 combined with low (filled) and high (open) light. Values represent the means ± SD ($n \geq 4$).

OA and high light affect photosynthetic performance of the tested species differently

Even though carbon fixation rates of Southern Ocean phytoplankton species with highly efficient CCMs are already close to saturation under present-day pCO_2 levels (Kranz et al. 2015, Trimborn et al. 2013, Young et al. 2015a, 2015b), lower energy expenditures as well as optimized resource allocation resulting from CCM downregulation may enable enhanced growth and/or carbon fixation rates at elevated pCO_2, particularly under saturating light intensities. In our tested species, C:N ratios remained constant with increasing pCO_2 and light (Fig. 1). Consistent with responses of the Antarctic diatoms *C. brevis* (Boelen et al. 2011) and *P. alata* (Hoogstraten et al. 2012a), our species did not benefit from OA and high light, but displayed no and/or negative CO_2 effects on growth and/or POC quota (Fig. 1). Compared with the prymnesiophyte *P. antarctica*, the two diatoms were more susceptible to OA in conjunction with high light. Under these conditions, maintenance of cellular stoichiometry was achieved in *C. debilis* at the expense of growth, being reduced by approximately 20% (Fig. 1). Interestingly, such reduction in growth was not observed when the same *C. debilis* strain was grown at a lower light intensity combined with OA (100 µmol m^{-2} s^{-1} and 1000 µatm pCO_2, Hoppe et al. 2015), indicating a negative effect on growth for *C. debilis* under OA with increasing light intensity. In comparison, cellular stoichiometry and growth were maintained in *F. kerguelensis* under OA combined with high light at the expense of biomass buildup. In this case, cellular contents of POC and PON were strongly reduced by 60% and 51%, respectively, whereas growth rates for this treatment remained unchanged (Fig. 1, PON data are not shown).

Elevated pCO_2 levels were previously found to cause a decline in growth and POC production in various temperate phytoplankton species due to a higher susceptibility to photo-damage (Chen and Gao 2011, Gao et al. 2012, McCarthy et al. 2012, Li and Campbell 2013). In fact, the acclimation to OA and high light decreased the maximum quantum yields of PSII (F_v/F_m) by 10 and 17% in *C. debilis* and *F. kerguelensis*, respectively (Fig. 2), indicating lowered photochemical efficiencies for both diatoms. This decline may potentially be the result of more strongly impaired PSII centers as previously observed in temperate diatom species (Gao et al. 2012, McCarthy et al. 2012, Wu et al. 2010). Diatoms were found to be prone for photoinactivation of their PSII reaction centers (Chen and Gao 2011, Gao et al. 2012, McCarthy et al. 2012, Li and Campbell 2013), implying an augmented capacity for PSII repair to maintain photosynthesis (McCarthy et al. 2012). Indeed, *C. debilis* showed highest concentrations of functional PSII reaction centers [RII] under high light conditions combined with ambient pCO_2 whereas when combined with elevated pCO_2 they were significantly reduced by 83% (Table 2), probably resulting from PSII photoinactivation. Opposed to *C. debilis*, irrespective of the pCO_2 *F. kerguelensis* was characterized by similar [RII] in both high

Table 3. Cellular concentrations of chlorophyll *a* (Chl *a*), chlorophyll c_2 (Chl c_2), fucoxanthin (Fuco), diadinoxanthin (Dd), and protective : light harvesting pigment ratios (Dt + Dt : Chl *a* + Chl c_2 + Fuco) were determined for *Phaeocystis antarctica*, *Chaetoceros debilis*, and *Fragilariopsis kerguelensis* acclimated to ambient and high pCO_2 combined with low and high light. Values were derived from at least four independent measurements.

Treatment	Chl *a* (fg cell^{-1})	Chl c_2 (fg cell^{-1})	Fuco (fg cell^{-1})	Dd (fg cell^{-1})	Protective: Light
P. antarctica					
390 LL	85 ± 10	10 ± 3	59 ± 10	5 ± 1	0.03 ± 0.00
390 HL	36 ± 5	3 ± 0	14 ± 3	11 ± 1	0.19 ± 0.03
800 LL	83 ± 13	12 ± 0	63 ± 6	5 ± 1	0.04 ± 0.01
800 HL	42 ± 4	3 ± 0	14 ± 4	11 ± 1	0.23 ± 0.02
C. debilis					
390 LL	182 ± 48	60 ± 20	202 ± 31	17 ± 2	0.04 ± 0.00
390 HL	21 ± 6	29 ± 20	34 ± 11	20 ± 5	0.24 ± 0.05
800 LL	139 ± 25	51 ± 19	187 ± 24	15 ± 4	0.04 ± 0.01
800 HL	53 ± 11	22 ± 9	60 ± 4	26 ± 2	0.21 ± 0.03
F. kerguelensis					
390 LL	79 ± 7	8 ± 1	37 ± 3	2 ± 1	0.02 ± 0.01
390 HL	200 ± 20	18 ± 3	86 ± 12	7 ± 1	0.02 ± 0.00
800 LL	87 ± 4	8 ± 1	43 ± 0	3 ± 0	0.02 ± 0.00
800 HL	55 ± 30	8 ± 6	54 ± 56	6 ± 4	0.03 ± 0.01

light treatments, suggesting higher costs to maintain similar numbers of functional PSII under elevated pCO_2, as previously observed for temperate diatoms (McCarthy et al. 2012, Li and Campbell 2013). In addition to this, values of ETR_{max}, which represent a measure for the maximum capacity for photosynthesis under saturating light (Schreiber et al. 1995), were significantly lowered by 29 and 83% in *C. debilis* and *F. kerguelensis*, respectively, under elevated pCO_2 and high light (Fig. 3, Table 2). The much stronger decline in ETR_{max} in *F. kerguelensis* resulted from reduced light-use efficiencies as indicated by the strongly diminished I_K and α under these conditions (Table 2). In comparison, I_K and α remained unaltered in *C. debilis*. A similar response was previously observed in the same *C. debilis* strain when grown at 100 µmol m^{-2} s^{-1} and 1000 µatm pCO_2 (Hoppe et al. 2015). The strongly impaired light-use efficiency in *F. kerguelensis* may be responsible to a large degree for the strong reduction in biomass production (Fig. 1), whereas this effect was not observed for *C. debilis*. Compared with the diatoms, the prymnesiophyte *P. antarctica* displayed no OA-dependent changes in ETR_{max}, I_K and α when grown under high light (Fig. 3, Table 2), its photosynthetic capacity remained unaltered, as shown by the unaltered F_v/F_m (Fig. 2), number of functional PSII reaction centers (Table 2) and POC quota (Fig. 1). Similarly, F_v/F_m as well as POC per cell remained unaffected under those conditions in the temperate prymnesiophyte *P. globosa* (Hoogstraten et al. 2012b). Hence, we can conclude that compared to the prymnesiophyte the two diatoms were more sensitive to OA in conjunction with high light.

To better understand the observed species-specific responses in ETR_{max} (Fig. 3, Table 2), we used the model by Kroon and Thoms (2006) to qualitatively assess the role of downregulation of electron transport on the production of adenosine triphosphate (ATP) vs nicotinamide adenine dinucleotide phosphate (NADPH). This ratio is determined by the number of protons (H^+) translocated across the thylakoid membrane per electron (e^-) transported through the electron transport chain. During linear electron transfer, H^+ is released by water splitting at PSII with a stoichiometry of 1 H^+/e^- at the luminal side of the chloroplast whereas during re-oxidation of plastoquinol at the cytochrome b6/f complex (involving the Q-cycle) this ratio is 2. Through cyclic electron transfer at the cytochrome b6/f, the H^+/e^- ratio can increase beyond the value of 3. Using the photosynthetic model of Kroon and Thoms (2006), the H^+/e^- ratio can be calculated as a function of irradiance. According to the model calculations, the H^+/e^- ratio was highest at limiting irradiance and decreased with increasing irradiance (Fig. 5). As 1 ATP molecule is generated per 3 or 4 H^+, the rate of ATP synthesis at a given rate of photochemistry is directly proportional to the H^+/e^- ratio. Hence, high H^+/e^- ratios favor ATP synthesis, in particular under low irradiance (Fig. 5). The model further revealed that the higher the rates of electron consumption in upstream metabolic reactions such as CO_2 fixation by RubisCO (these processes are collectively represented by the rate constant of ferredoxin re-oxidation in the model) the more pronounced was the decline of the H^+/e^- ratio (Fig. 5). Hence, the strongly lowered ETR_{max} by 83% under OA and high light in *F. kerguelensis* (Fig. 3, Table 2) suggests a smaller rate constant of ferredoxin re-oxidation, causing a high H^+/e^- ratio (Fig. 5). Congruently, downregulation of ETRs can increase the rate of ATP synthesis relative

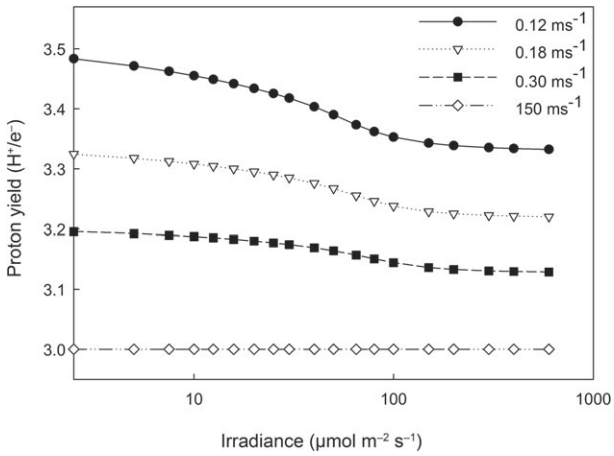

Fig. 5. Theoretical simulations of the proton yield (H^+/e^- ratio) as a function of irradiance based on the model of Kroon and Thoms (2006) using the antenna scenario 2 (see Table 2 in Kroon and Thoms 2006). The value for the rate constant of ferredoxin re-oxidation, which represents the e^- consumption in upstream metabolic reactions, was increased from 0.12 to 150 ms^{-1}.

to the rate of NADPH synthesis precluding thereby ATP limitation under OA and high light conditions. Lowered rates of ATP synthesis relative to the rate of NADPH synthesis can decrease the capacity to take up nutrients (especially nitrate), potentially lowering protein synthesis and carbon fixation (owing to a depressed conversion of carbohydrate skeletons to protein), as seen by the reduced POC quota while the C:N ratio was kept constant in *F. kerguelensis* under OA and high light (Fig. 1). In comparison to *F. kerguelensis*, under these conditions the decline in ETR_{max} was much less pronounced in *C. debilis* (29%) whereas ETR_{max} remained unchanged in *P. antarctica* (Fig. 3, Table 2). As a consequence of the low synthesis rate of ATP, transport of excess NADPH out of the chloroplast may be required to produce NADH in the cytosol. Subsequently, the rate of ATP synthesis might potentially increase inside the mitochondria consuming the extra NADH from the cytosol. By this mechanism, the overall ATP/NADPH ratio could be increased in *C. debilis* and *P. antarctica* while their photosynthetic ETRs remained still high. Using the photosynthetic model of Kroon and Thoms (2006), the observed species-specific differences in photosynthetic performance in response to OA and high light can be explained in terms of different species-specific strategies for tuning the available flux of ATP and NADPH. Both strategies, downregulation of the photosynthetic electron transport and/or transport of excess NADPH out of the chloroplast, may explain why our tested species did not benefit from OA at high light, but rather displayed no and/or negative effects on cellular POC contents (Fig. 1A–C).

To diminish light absorption and therewith the potential for photoinhibition under high light conditions as previously observed for diatoms and prymnesiophytes (Arrigo et al. 2010, Kropuenske et al. 2010, Van Leeuwe et al. 2005), cellular chlorophyll *a* (Chl *a*) contents were generally reduced in high compared with low light acclimated cells of *P. antarctica* and *C. debilis* (Table 3). Exposed to high light in conjunction with OA, Chl *a* per cell remained unchanged in *P. antarctica*, as previously observed in *P. globosa* (Hoogstraten et al. 2012b), whereas cellular Chl *a* contents were, unexpectedly, enhanced in *C. debilis* (Table 3). Correspondingly, also the light harvesting pigment concentration of fucoxanthin (Fuco) was increased under those conditions (Table 3). In agreement with this, an OA-dependent induction of chlorophyll-fucoxanthin protein genes was reported for the temperate diatom *P. tricornutum* (Li et al. 2015). Such photoacclimation response by *C. debilis* may be a strategy to maximize light harvesting to counteract the observed reduced photochemical efficiency through the lowered number of functional PSII. In contrast to *C. debilis*, *F. kerguelensis* displayed the reverse trend in cellular Chl *a* concentrations in response to high light, with very high and low concentrations under ambient and elevated pCO_2, respectively (Table 3). Besides Chl *a* per cell (Table 3), also ETR_{max} (Table 2) and POC per cell (Fig. 1) were strongly increased to achieve maximum light absorption, electron transport and biomass build-up under ambient pCO_2 and high-light conditions. Under high light and OA, however, cellular Chl *a* contents were strongly reduced, resulting further in impaired light-use efficiency (Table 2) and reduced biomass build-up (Fig. 1) for *F. kerguelensis*. As previously observed for this species (Trimborn et al. 2014), the acclimation to high light and elevated pCO_2 further led to an increased disconnection of antennae from PSII reaction centers from ambient to high pCO_2 levels (Table 2), pointing toward a reduced capacity of transferring excitons to the PSII reaction centers, hampering therefore the efficiency of PSII. Hence, the synergistic effect by high light and OA strongly impaired the photosynthetic capacity of *F. kerguelensis*, with negative effects for biomass production.

Next to adjustment of cellular light harvesting pigmentation, concentrations of photoprotective pigments such as Dt and Dd for the dissipation of excess light energy are usually found to increase with increasing light intensity in diatoms and prymnesiophytes (Kropuenske et al. 2010, Van Leeuwe et al. 2005). As expected, the contribution of photoprotective (sum of cellular contents of Dd and Dt) relative to light harvesting pigment concentrations (sum of cellular contents of Chl *a*, Chl c_2, Fuco) increased with increasing light intensity in the three

tested species (Table 3). Moreover, changes in pCO_2 did not affect the ratio of photoprotective relative to light harvesting pigments in the high light treatments in any of the tested species (Table 3). Correspondingly, NPQ values were similar under high light in *P. antarctica* and *C. debilis* irrespective of the pCO_2 (at highest around 2, Fig. 4). In line with this, no CO_2-dependent effect on NPQ was previously observed in the same two species when grown at 100 µmol m^{-2} s^{-1} (180 and 1000 µatm pCO_2 Trimborn et al. 2014). For high light-acclimated cells of *F. kerguelensis*, however, NPQ was differently affected by pCO_2. When acclimated to ambient pCO_2, for *F. kerguelensis* calculated NPQ remained low or even negative with increasing irradiances (at highest ~0.5), indicating potentially an altered redox status of intersystem electron transport under these conditions (Bailleul et al. 2015), disrupting the underlying assumptions for estimation of NPQ. In contrast under elevated pCO_2, NPQ increased with increasing irradiances (at highest around 3, Fig. 4), suggesting enhanced dissipation of excess energy under OA and high light conditions. Compared with *P. antarctica* and *C. debilis*, only *F. kerguelensis* was characterized by a significantly reduced ability to recover from short-term light stress (yield recovery measured after FLC-curves, Fig. 2) under high light and OA, indicating once more its higher susceptibility for photo-damage.

Implications for future diatom and prymnesiophyte occurrence and biogeochemical cycling

As diatoms and prymnesiophytes are generally considered key drivers of biogeochemical cycling, with diatoms predominantly regulating the carbon (Smetacek 1999) and silicon cycle (Tréguer 2002) and *P. antarctica* the marine sulfur cycle (Liss et al. 1994), it is crucial to understand how both taxonomic groups will respond to the different future OA and light scenarios. Strong species-specific differences in the ability to cope with changing light and CO_2 conditions were observed among the three species. The prymnesiophyte *P. antarctica* was found to be most tolerant, displaying no negative effects on growth or carbon fixation under all experimental conditions (Fig. 1). Owing to its efficient photoacclimation strategy (Table 2 and 3), it was not susceptible for photo-damage in any scenario (Fig. 2). Only after exposure to short-term light stress, *P. antarctica* was characterized by lowered yield recovery compared with the two diatoms in the tested scenarios (Fig. 2). As previously observed for *P. antarctica* (Arrigo et al. 2010, Kropuenske et al. 2010, Mills et al. 2010), it does not cope well under conditions of prolonged high light stress. Interestingly, this response was observed irrespective of the applied CO_2 scenario, pointing out its tolerance to OA.

In contrast to the prymnesiophyte, photochemical efficiencies of both diatoms were enhanced under low relative to high light, irrespective of the pCO_2 scenario (Fig. 2). This finding suggests that both diatoms generally benefitted from the favorable low light conditions potentially through a reduced need for PSII repair and subsequently lowered energetic expenditures. On the other hand, they also showed higher capacities for yield recovery than *P. antarctica* following short-term high light exposure (Fig. 2), indicating efficient strategies of both diatoms to dissipate excess light on short time scales. However, photoprotection strategies differed between both diatoms. While the high potential for yield recovery of *F. kerguelensis* cannot be explained on the basis of our data, *C. debilis* on the other hand was found to possess higher Dd per cell than *P. antarctica* (Table 2), which is in line with previous observations for *F. cylindrus* and *C. brevis* (Kropuenske et al. 2010, Van de Poll et al. 2011). Hence, our data support previous observations and confirm a pronounced ability of the two diatoms to counteract high light stress on short time scales. This ability was, however, impaired in response to OA as none of the applied OA-light scenarios caused stimulation in growth or carbon fixation in both diatoms.

Overall, this study revealed that the physiological responses to OA and light of the tested three Southern Ocean phytoplankton species strongly differed. Although it is difficult to predict how Southern Ocean phytoplankton species will respond to the future climatic scenarios, it is obvious from this study that OA and changes in light availability had no beneficial effects on any of the tested species. The prymnesiophyte *P. antarctica* could be favored over the two diatoms under the projected OA-light scenarios. As the biological carbon pump is primarily driven by diatoms, lower diatom abundances in combination with reduced biomass build-up by diatoms could potentially weaken the biological carbon pump, representing a positive feedback to rising atmospheric CO_2.

Author contributions

Sc. T. designed the experiments. T. B. and Sc. T. performed the experiments. Sc. T., T. B., Si. T. and J. P. H. analyzed the data. Sc. T., S. B., Si. T. and K. B. interpreted and wrote the paper.

Acknowledgements – Sc. T., T. B. and J. P. H. were funded by the Helmholtz Impulse Fond (HGF Young Investigators Group *EcoTrace*). S. B. was funded by the Deutsche Forschungsgemeinschaft (DFG) in the framework of the

priority program '*Antarctic Research with comparative investigations in Arctic ice areas*', grant no.: BE5105/1-1.

References

Arrigo KR, Mills MM, Kropuenske LR, van Dijken GL, Alderkamp A-C, Robinson DH (2010) Photophysiology in two major Southern Ocean phytoplankton taxa: photosynthesis and growth of *Phaeocystis antarctica* and *Fragilariopsus cylindrus* under different irradiance levels. Integr Comp Biol 50: 950–966

Bailleul B, Berne N, Murik O, Petroutsos D, Prihoda J, Tanaka A, Villanova V, Bligny R, Flori S, Falconet D, Krieger-Liszkay A, Santabarbara S, Rappaport F, Joliot P, Tirichine L, Falkowski PG, Cardol P, Bowler C, Finazzi G (2015) Energetic coupling between plastids and mitochondria drives CO_2 assimilation in diatoms. Nature 524: 366–369

Beardall J, Raven JA (2013) Limits to phototrophic growth in dense culture: CO_2 supply and light. In: Borowitzka MA, Moheimani NR (eds) Algae for Biofuels and Energy. Springer, Dordrecht, pp 91–97

Boelen P, van de Poll WH, van der Strate HJ, Neven IA, Beardall J, Buma AGJ (2011) Neither elevated nor reduced CO_2 affects the photophysiological performance of the marine Antarctic diatom *Chaetoceros brevis*. J Exp Mar Biol Ecol 406: 38–45

Brewer PG, Bradshow AL, Williams RT (1986) Measurement of total carbon dioxide and alkalinity in the North Atlantic Ocean in 1981. In: Trabalka JR, Reichle DE (eds) The Changing Carbon Cycle – A Global Analysis. Springer, New York City, New York, USA, pp 358–381

Chen S, Gao KS (2011) Solar ultraviolet radiation and CO_2-induced ocean acidification interacts to influence the photosynthetic performance of the red tide alga *Phaeocystis globosa* (Prymnesiophyceae). Hydrobiologia 675: 105–117

Dickson AG, Millero FJ (1987) A comparison of the equilibrium constants for the dissociation of carbonic acid in seawater media. Deep-Sea Res 34: 1733–1743

Gao K, Campbell DA (2014) Photophysiological responses of marine diatoms to elevated CO_2 and decreased pH: a review. Funct Plant Biol 41: 449–459

Gao K, Xu J, Gao G, Li Y, Hutchins DA, Huang B, Wang L, Zheng Y, Jin P, Cai X, Häder D-P, Li W, Xu K, Liu N, Riebesell U (2012) Rising CO_2 and increased light exposure synergistically reduce marine primary productivity. Nat Clim Change 2: 519–523

Genty B, Briantais J-M, Baker NR (1989) The relationship between the quantum yield of photosynthetic electron transport and quenching of chlorophyll fluorescence. Biochim Biophys Acta 990: 87–92

Giordano M, Beardall J, Raven JA (2005) CO_2 concentrating mechanisms in algae: mechanisms, environmental modulation, and evolution. Annu Rev Plant Biol 56: 99–131

Gran G (1952) Determinations of the equivalence point in potentiometric titrations of seawater with hydrochloric acid. Oceanol Acta 5: 209–218

Guillard RRL, Ryther RH (1962) Studies of marine planktonic diatoms. Can J Microbiol 8: 229–239

Hauck J, Völker C, Wolf-Gladrow DA, Laufkötter C, Vogt M, Aumont O, Bopp L, Buitenhuis ET, Doney SC, Dunne J, Gruber N, Hashioka T, John J, Le Quéré C, Lima ID, Nakano H, Séférian R, Totterdell IJ (2015) On the Southern Ocean CO_2 uptake and the role of the biological carbon pump in the 21st century. Glob Biogeochem Cycle 29: 1451–1470

Hoogstraten A, Timmermans KR, de Baar HJW (2012a) Morphological and physiological effects in *Proboscia alata* (Bacillariophyceae) grown under different light and CO_2 conditions of the modern Southern Ocean. J Phycol 48: 559–568

Hoogstraten A, Peters M, Timmermans KR, de Baar HJW (2012b) Combined effects of inorganic carbon and light on *Phaeocystis globosa* Scherffel (Prymnesiophyceae). Biogeoscience 9: 1885–1896

Hopkinson BM, Dupont CL, Allen AE, Morel FMM (2011) Efficiency of the CO_2-concentrating mechanism of diatoms. Proc Natl Acad Sci USA 108: 3830–3837

Hoppe CJM, Holtz L, Trimborn S, Rost B (2015) Ocean acidification decreases the light use efficiency in an Antarctic diatom under dynamic but not constant light. New Phytol 207: 159–171

Kolber ZS, Prásîl O, Falkowski PG (1998) Measurements of variable chlorophyll fluorescence using fast-repetition rate techniques: defining methodology and experimental protocols. Biochim Biophys Acta 1367: 88–106

Kranz SA, Levitan O, Richter K-U, Prásil O, Berman-Frank I, Rost B (2010) Combined effects of CO_2 and light on the N_2-fixing cyanobacterium Trichodesmium IMS101: physiological responses. Plant Physiol 154: 334–345

Kranz SA, Young JN, Hopkinson BM, Goldman JAL, Tortell PD, Morel FMM (2015) Low temperature reduces the energetic requirement for the CO_2 concentrating mechanism in diatoms. New Phytol 205: 192–201

Kroon B, Thoms S (2006) From electron to biomass: a mechanistic model to describe phytoplankton photosynthesis and steady-state growth rates. J Phycol 42: 593–609

Kropuenske LR, Mills MM, Van Dijken GL, Alderkamp A-C, Berg GM, Robinson DH, Welschmeyer NA, Arrigo KR (2010) Strategies and rates of photoacclimation in two major Southern Ocean phytoplankton taxa: *Phaeocystis antarctica* (Haptophyta) and *Fragilariopsis cylindrus* (Bacillariophyceae). J Phycol 50: 950–966

Li G, Campbell DA (2013) Rising CO_2 interacts with growth light and growth rate to alter photosystem II

photoinactivation of the coastal diatom *Thalassiosira pseudonana*. PLoS One 8: e55562
Li Y, Xu J, Gao K (2014) Light-modulated responses of growth and photosynthetic performance to ocean acidification in the model diatom *Phaeodactylum tricornutum*. PLoS One 9: e96173
Li Y, Zhuang S, Wu Y, Ren H, Cheng F, Lin X, Wang K, Beardall J, Gao K (2015) Ocean acidification modulates expression of genes and physiological performance of a marine diatom. Biogeosci Discuss 12: 15809–15833
Liss PS, Malin G, Turner SM, Holligan PM (1994) Dimethylsulphide and *Phaeocystis*: a review. J Mar Syst 5: 1–4
Mackey KRM, Morris JJ, Morel FMM, Kranz SA (2015) Response of photosynthesis to ocean acidification. Oceanography 28: 74–91
McCarthy A, Rogers SP, Duffy SJ, Campbell DA (2012) Elevated carbon dioxide differentially alters the photophysiology of *Thalassiosira pseudonana* (Bacillariophyceae) and *Emiliania huxleyi* (Haptophyta). J Phycol 48: 635–646
Mehrbach C, Culberson C, Hawley J, Pytkovicz R (1973) Measurement of the apparent dissociation constants of carbonic acid in seawater at atmospheric pressure. Limnol Oceanogr 18: 897–907
Mills MM, Kropuenske LR, van Dijken GL, Alderkamp A-C, Berg GM, Robinson DH, Welschmeyer NA, Arrigo KR (2010) Photophysiology in two Southern Ocean phytoplankton taxa: photosynthesis of *Phaeocystis antarctica* (Prymnesiophyceae) and *Fragilariopsis cylindrus* (Bacillariophyceae) under simulated mixed-layer irradiance. J Phycol 46: 1114–1127
Murata N, Takahashi S, Nishiyama Y, Allakhverdiev SI (2007) Photoinhibition of photosystem II under environmental stress. Biochim Biophys Acta 1767: 414–421
Oxborough K (2012) FastPro8 GUI and FRRf3 Systems Documentation. Chelsea Technologies Group Ltd, West Molesey, UK
IPCC (2014) Pachauri RK, Meyer LA (eds) Climate Change 2014: Synthesis Report Basis, Contribution of working groups I, II and III to the fifth assessment. IPCC, Geneva
Pierrot DE, Lewis E, Wallace DWR (2006) MS Excel program developed for CO_2 system calculations. Available at http://cdiac.ornl.gov/ftp/co2sys (accessed 12 July 2013)
Ralph PJ, Gademann R (2005) Rapid light curves: a powerful tool to assess photosynthetic activity. Aquat Bot 82: 222–237
Raven JA (2011) The cost of photoinhibition. Physiol Plant 142: 87–104
Raven JA, Giordano M, Beardall J, Maberly SC (2011) Algal and aquatic plant carbon concentrating mechanisms in relation to environmental change. Photosynth Res 109: 281–296
Redfield AC (1958) The biological control of chemical factors in the environment. Am Sci 64: 205–221
Riebesell U, Wolf-Gladrow DA, Smetacek V (1993) Carbon dioxide limitation of marine phytoplankton growth rates. Nature 361: 249–251
Robinson DH, Kolber Z, Sullivan CW (1997) Photophysiology and photoacclimation in surface sea ice algae from McMurdo Sound, Antarctica. Mar Ecol Prog Ser 147: 243–256
Rokitta SD, Rost B (2012) Effects of CO_2 and their modulation by light in the life-cycle stages of the coccolithophore *Emiliania huxleyi*. Limnol Oceanogr 57: 607–618
Schreiber U, Bilger W, Neubauer C (1995) Chlorophyll fluorescence as a nonintrusive indicator for rapid assessment of in vivo photosynthesis. In: Schulze ED, Caldwell MM (eds) Ecophysiology of Photosynthesis. Springer, Berlin, pp 49–70
Smetacek V (1999) Diatoms and the carbon cycle. Protist 150: 25–32
Suggett DJ, MacIntyre HL, Geider RJ (2004) Evaluation of biophysical and optical determinations of light absorption by photosystem II in phytoplankton. Limnol Oceanogr Method 2: 316–332
Suggett DJ, MacIntyre HL, Kana TM, Geider RJ (2009) Comparing electron transport with gas exchange: parameterising exchange rates between alternative photosynthetic currencies for eukaryotic phytoplankton. Aquat Microb Ecol 56: 147–162
Torstensson A, Hedblom M, Andersson J, Andersson MX, Wulff A (2013) Synergism between elevated pCO_2 and temperature on the Antarctic sea ice diatom *Nitzschia lecointei*. Biogeosciences 10: 6391–6401
Torstensson A, Hedblom M, Mattsdotter Björk M, Chierici M, Wulff A (2015) Long-term acclimation to elevated pCO_2 alters carbon metabolism and reduces growth in the Antarctic diatom *Nitzschia lecointei*. Proc R Soc B 282: 20151513
Tréguer P (2002) Silica and the cycle of carbon in the Ocean. Geoscience 334: 3–11
Trimborn S, Brenneis T, Sweet E, Rost B (2013) Sensitivity of Antarctic phytoplankton species to ocean acidification: growth, carbon acquisition and species interaction. Limnol Oceanogr 58: 997–1007
Trimborn S, Thoms S, Petrou K, Kranz S, Rost B (2014) Photophysiological responses of Southern Ocean phytoplankton to changes in CO_2 concentrations: short-term versus acclimation effects. J Exp Mar Biol Ecol 451: 44–54
Utermöhl H (1958) Zur Vervollkommung der quantitativen Phytoplankton-Methodik. Mitt/Int Ver Theoret Angewan Limnol 9: 1–38

Van de Poll W, Lagunas M, de Vries T, Visser RJW, Buma AGJ (2011) Non-photochemical quenching of chlorophyll fluorescence and xanthophyll cycle responses after excess PAR and UVR in *Chaetoceros brevis*, *Phaeocystis antarctica* and coastal Antarctic phytoplankton. Mar Ecol Prog Ser 426: 119–131

Van Leeuwe MA, van Sikkelerus B, Gieskes WWC, Stefels J (2005) Taxon specific differences in photoacclimation to fluctuating irradiance in an Antarctic diatom and a green flagellate. Mar Ecol Prog Ser 288: 9–19

Young EB, Beardall J (2005) Modulation of photosynthesis and inorganic carbon acquisition in a marine microalga by nitrogen, iron, and light availability. Can J Bot 83: 917–928

Young JN, Kranz SA, Goldman JAL, Tortell PD, Morel FMM (2015a) Antarctic phytoplankton down-regulate their carbon-concentrating mechanisms under high CO_2 with no change in growth rates. Mar Ecol Prog Ser 532: 13–28

Young JN, Goldman JAL, Kranz SA, Tortell PD, Morel FMM (2015b) Slow carboxylation of Rubisco constrains the rate of carbon fixation during Antarctic phytoplankton blooms. New Phytol 205: 172–181

Wright SW, Jeffrey SW, Manoura RFC, Llewellyn CA, Bjornland T, Repeta D, Welschmeyer N (1991) Improved HPLC method for the analysis of chlorophylls and carotenoids from marine phytoplankton. Mar Ecol Prog Ser 77: 183–196

Wu Y, Gao K, Riebesell U (2010) CO_2-induced seawater acidification affects physiological performance of the marine diatom *Phaeodactylum tricornutum*. Biogeosci 7: 2915–2923

Edited by W. S. Chow